

# Self-Repairing Learning Rule for Spiking Astrocyte-Neuron Networks

Junxiu Liu<sup>1</sup>, Liam J. McDaid<sup>1</sup>, Jim Harkin<sup>1</sup>, John J. Wade<sup>1</sup>, Shvan Karim<sup>1</sup>,  
Anju P. Johnson<sup>2</sup>, Alan G. Millard<sup>2</sup>, David M. Halliday<sup>2</sup>, Andy M. Tyrrell<sup>2</sup>,  
and Jon Timmis<sup>2</sup>

<sup>1</sup> School of Computing and Intelligent Systems, Ulster University,  
Northern Ireland, United Kingdom, BT48 7JL  
{j.liu1,lj.mcdaid,jg.harkin,jj.wade,haji\_karim-s}@ulster.ac.uk  
<sup>2</sup> Department of Electronic Engineering, University of York,  
York, United Kingdom, YO10 5DD  
{anju.johnson,david.halliday,alan.millard,  
andy.tyrrell,jon.timmis}@york.ac.uk

**Abstract.** In this paper a novel self-repairing learning rule is proposed which is a combination of the spike-timing-dependent plasticity (STDP) and Bienenstock, Cooper, and Munro (BCM) learning rules: in the derivation of this rule account is taken of the coupling of GABA interneurons to the tripartite synapse. The rule modulates the plasticity level by shifting the plasticity window, associated with STDP, up and down the vertical axis as a function of postsynaptic neural activity. Specifically when neurons are inactive, the window is shifted up the vertical axis (open) and as the postsynaptic neuron activity increases and, as learning progresses, the plasticity window moves down the vertical axis until learning ceases. Simulation results are presented which show that the proposed approach can still maintain the network performance even with a fault density approaching 80% and because the rule is implemented using a minimal computational overhead it has potential for large scale spiking neural networks in hardware.

**Keywords:** Astrocyte-neuron network, learning window, self-repair, fault tolerance

## 1 Introduction

Spiking neural networks (SNNs) use models derived from the spike timing of neurons to encode and process information. Recent research has demonstrated the advantages of these computing paradigms in modelling memory [1], pattern recognition [2], fault tolerance [3] and also in many other applications [4, 5]. Astrocytes have been shown to co-exist with neurons [6] where these cells communicate with synapses and neurons, and in doing so, regulate synaptic morphology and formation [6]. Artificial astrocyte cells together with spiking neurons form an astrocyte-neuron network (S-ANN) which facilitates a distributed and

fine-grained self-repair capability. The authors have proposed this self-repairing mechanism in an earlier paper [7] and also applied it to hardware systems with the aim of enhancing the fault-tolerant capability of the system [8, 9]. In these papers, the pre-synaptic terminal receives the feedback signals from the post-synaptic neuron and astrocyte cell, respectively, which modulate the probability of release (PR) of all synapses associated with the postsynaptic neuron. For example, if synapses are damaged to such an extent that postsynaptic neural activity ceases, then other undamaged synapses will be potentiated by the astrocyte cell until the neural activity is restored (repair) [7].

In this paper, we go further and propose a novel self-repairing learning rule that uses recent evidence [7] to explain how the spike-timing-dependent plasticity (STDP) and Bienenstock, Cooper, and Munro (BCM) learning rules co-exist to give a learning function that is under the control of postsynaptic neuron activity. The key novelty in this work is that we now couple a GABA interneuron with tripartite synapses and show that this interaction can implement a presynaptic frequency selectivity capability through modulation of PR at synaptic sites, and that the PR parameter is also under the control of the postsynaptic firing activity: modulation of PR by postsynaptic activity underpins self-repair. The rest of paper is organized by follows. Section 2 presents the self-repairing learning rule in detail. Section 3 gives the simulation results and section 4 concludes the paper.

## 2 Self-repairing learning rule

This section discusses the biophysical interactions that occur at the tripartite synapse in the presence of GABA interneurons and subsequently shows how such interactions can be interpreted to give rise to a self-repairing capability.

### 2.1 Activity-dependent mechanism in the S-ANNs

Fig. 1 represents the signalling pathways between a GABA interneuron and the tripartite synapse [10] at a low presynaptic frequency (A) and at a high presynaptic frequency (B). The conventional tripartite synapse consists of a presynaptic terminal, a postsynaptic terminal, and an astrocyte terminal. However, we now consider the new additional signalling pathways between these terminals and a GABA interneuron terminal. Note also that we are taking the presynaptic spiking frequency ( $f_{pre}$ ) to be the same as that of the GABA neuron [10].

At low  $f_{pre}$  GABA binds to GABA-A receptors on the presynaptic terminal and to GABA-B receptors on the astrocyte (Fig. 1A). However, because of inositol 1, 4, 5-trisphosphate ( $IP_3$ ) degradation within the astrocyte an insufficient amount of GABA is released to open calcium stores in the astrocyte at low  $f_{pre}$  and therefore there is no gliotransmitter release from the astrocyte. Consequently because GABA is binding to GABA-A receptors at the presynaptic terminal under low  $f_{pre}$ , then this has an inhibitory effect represented as a low PR value (Fig. 1A). However, if  $f_{pre}$  is increased (Fig. 1B), a point is reached

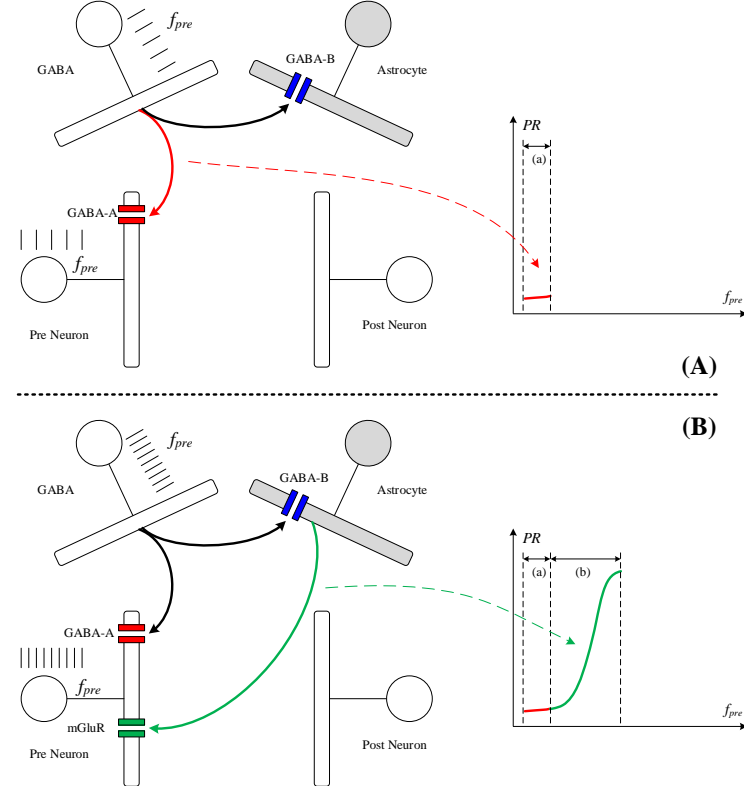


**Fig. 1.** Tripartite synapse coupled to a GABA interneuron under low (A) and high (B) presynaptic firing.

whereby a sufficient amount of  $IP_3$  exists within the astrocyte to trigger the opening of the calcium store and in this case gliotransmitter is released and binds to group I metabotropic Glutamate Receptors (mGluR) on the presynaptic receptors. This overrides the inhibitory effect and causes a rapid increase in PR at the presynaptic terminal, as shown in Fig. 1B. However, if  $f_{pre}$  continues to increase the  $IP_3$  within the astrocyte increases and an upper threshold level is reached whereby the calcium oscillations stop and the release of gliotransmitter by the astrocyte ceases. This causes a fall-off in PR as shown in Fig. 2. Therefore, inhibitory GABA interneurons coupled to tripartite synapses appear to give rise to a frequency filtering effect where the effective passband is a function of cell morphology, receptor density and other factors.

To minimise the computational overhead we describe the relationship between the spike frequency ( $f_{pre}$ ) and synaptic PR using a Gaussian function, as per Fig. 2, with the three stages of (a)-(c) as described above.

The Gaussian curve is described by

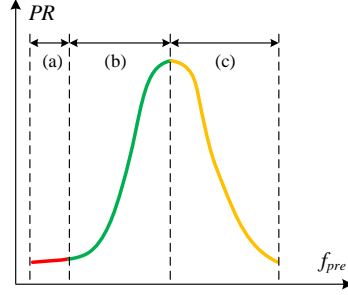


**Fig. 2.** PR vs  $f_{pre}$  for a tripartite synapse and GABA interneuron.

$$PR = e^{-\frac{(f_{pre} - f_s)^2}{2\sigma^2}}, \quad (1)$$

where  $f_s$  is the centre frequency and  $\sigma$  is the width of the Gaussian passband.

## 2.2 Self-repairing learning rule

In this paper, the Leaky Integrate-and-Fire (LIF) neuron model [11] is employed due to its relatively low computing and minimal parameter tuning requirements. It is given by

$$\tau_m \frac{dv}{dt} = -v(t) + R_m \sum_{i=1}^n I_{syn}^i(t), \quad (2)$$

where  $\tau_m$  is the neuron membrane time constant,  $v$  is the neuron membrane potential,  $R_m$  is the membrane resistance,  $I_{syn}^i$  is the current injected to the neuron membrane by  $i^{th}$  synapse, and  $n$  is the total number of synapses associated with the neuron. When the neuron membrane potential  $v$  is greater than the firing threshold value  $v_{th}$ , the neuron fires and outputs a spike. Subsequently, it goes to the reset state and remains for the duration of the refractory period ( $\sim 2$ ms).

To implement a self-repairing mechanism for the S-ANN, a learning algorithm needs to be designed. In this approach, the STDP [12, 13], together with BCM learning rule [14, 15], are combined to develop the BCM-STDP rule. STDP uses the time difference between presynaptic and postsynaptic spikes to adjust the synaptic weights, where the equations in (3) cause long-term potentiation (LTP) for  $\Delta t \leq 0$  and long-term depression (LTD) for  $\Delta t > 0$ . In this approach, potentiation/depression is described by

$$\delta w(\Delta t) = \begin{cases} A_0 \exp(\frac{\Delta t}{\tau_+}), & \Delta t \leq 0 \\ -A_0 \exp(\frac{\Delta t}{\tau_-}), & \Delta t > 0 \end{cases} \quad (3)$$

where  $\delta w(\Delta t)$  is the weight update,  $\Delta t$  is the time difference between presynaptic and postsynaptic spike events,  $A_0$  is the height of STDP learning window controlling the maximum levels of weight potentiation and depression,  $\tau_+$  and  $\tau_-$  control the decay rate of weight updating for potentiation and depression, respectively. A symmetrical plasticity window is assumed and  $\tau_+ = \tau_- = 40ms$ .

In addition, the BCM learning rule modulates the height of the STDP plasticity window as a function of the actual firing rate of neuron according to

$$A_0 = \frac{A}{1 + e^{a(f-f_o)}} - A_- \quad (4)$$

where  $f$  and  $f_o$  are the actual and target firing rates of the postsynaptic neuron, respectively.  $A$  is the maximum height of plasticity window and  $A_-$  is the maximum height of the plasticity window for depression. The parameter  $a$  is constant which controls the opening/closing speed of the plasticity window and is found experimentally to be 0.1.

While the model in (4) does not capture the detailed biophysical processes underpinning the functional relationship between postsynaptic neural activity and the level of plasticity, we offer up here a plausible explanation for this. In a recent paper [7] it was shown that the endocannabinoid retrograde signaling pathways cause the level of  $IP_3$  within astrocytes to increase (the indirect pathway) due to postsynaptic activity. Therefore, if  $f_{pre}$  is such that the PR value is maximum (see Fig. 2) then the  $IP_3$  level within the astrocyte is between a lower and upper threshold limit and a calcium wave results. Under this condition and with little or no postsynaptic neural activity, the level of  $IP_3$  will remain unchanged and PR will be at its maximum level (high level of plasticity). However, as learning progresses and the postsynaptic activity increases the indirect retrograde pathway strengthens causing the level of  $IP_3$  within the astrocyte to increase and with sufficiently high postsynaptic activity (after a period of learning) the level of  $IP_3$  moves above the upper threshold and the calcium wave ceases resulting in a falloff in PR (low level of plasticity). Hence it is proposed in this work that the retrograde signaling pathway may be the link between neural activity and the level of plasticity as proposed in the BCM rule. However, the authors are currently exploring this retrograde signaling pathway further to distill out a more detailed and biophysical based model, which will be the subject of a subsequent publication.

### 3 Results

This section presents simulation results where, in Fig. 3, the S-ANN includes two presynaptic neurons (N1 and N2), a postsynaptic neuron (N3) and two astrocyte cells connecting to the synapses. Each pre-post neural coupling has multiple synaptic pathways (8 in total) where each pathway is assumed to be of morphology modelled by a different delay: each synaptic pathway is delayed from its neighbour by 2 ms and therefore with a minimum delay of zero, the maximum delay of a pathway is 14 ms. As presented in section 2.1, astrocyte cell modulates

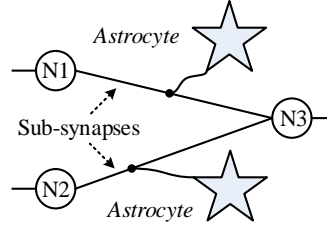


**Fig. 3.** An S-ANN with three neurons and two astrocyte cells.

the synaptic transmission and determines the activities of postsynaptic neurons. In this experiment, we are using an input Poisson spike train for both presynaptic neurons and the centre frequency for all “filter” synapses is 25 Hz, i.e. when  $f_{pre}=25$  Hz, PR is maximum. The target frequency of N3 is also set to 25 Hz. The performance of this S-ANN is analysed under two different conditions. The first condition is a healthy S-ANN with different input patterns, through which the pattern recognition capability of the network can be evaluated. The second condition is a faulty S-ANN where several synapses are damaged and the self-repairing mechanism of the S-ANN will be evaluated.

### 3.1 No faults

Two input spike trains (25 Hz) are used to test the network performance under the no fault condition. As a 25 Hz spike train is compatible with the center frequency of the filter synapses we anticipate that a normal learning phase will occur with the postsynaptic target frequency also set to 25 Hz. Fig. 4 shows the results of output spike frequency of N3 under the above conditions and, as can be seen, the spike frequency of N3 increases gradually during the training phase and eventually stabilizes at 25 Hz after  $\sim 60$  seconds. Fig. 5 shows the results of synaptic weights which as expected, show a slow potentiation over the learning period and stabilizes at  $\sim 80$  seconds. Additional simulations (not shown) were carried out with presynaptic spike train frequencies outside the filter window and showed that no learning occurred, which verified that our network was selective to the input spike train patterns centered at or close to 25 Hz.

### 3.2 Partial faults

To evaluate the self-repairing capability of the proposed S-ANN, the spike train frequency of both N1 and N2 were again set to the center frequency of the Gaussian curve ( $=25$  Hz) and the S-ANN was trained as before (see Fig. 6) with a target frequency of 25 Hz for N3. However, after a normal training period had finished (200 seconds) 6 of the 8 synapses connecting N2 to N3 were broken (PR was forced low) which represents a fault density of 75%. Fig. 6 shows the activity of N3 diminishes at 200 seconds where its activity drops to  $\sim 17$  Hz

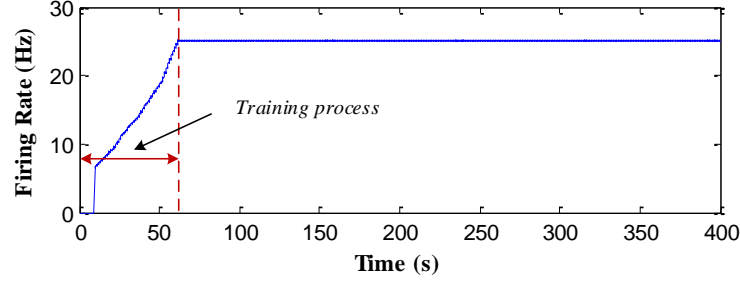


**Fig. 4.** Firing rate of N3 under the condition of no faults.

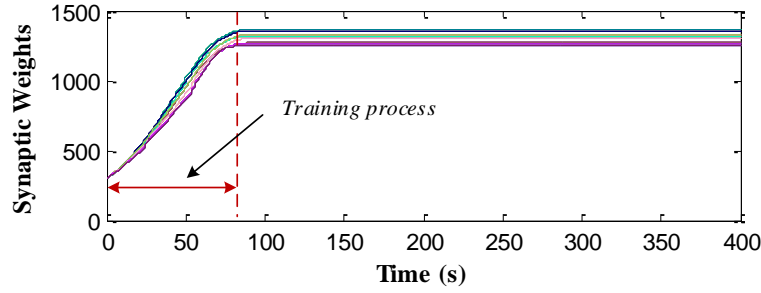


**Fig. 5.** Synaptic weights under the condition of no faults.

due to the impact of the faults. From time 200 seconds the learning window re-opens and the training process then restarts and the healthy synapses have their PR increased. Fig. 7 shows the synapse re-training or adjustment. This process of retraining the network to recover the firing rate of N3 defines the self-repairing process. It can be seen that the synaptic weights of the remaining healthy synapses potentiate further within a time frame of  $\sim 75$  seconds and the firing rate of N3 recovers in a little under 60 seconds (see Fig. 6) to the pre-fault value. Based on this self-repairing mechanism, even when the faults occur and the synaptic connections are damaged, the network still retains the capability to reorganize itself by re-training and consequently recover to the pre-fault mapping. This is a very important capability for the fault-tolerant hardware systems due to the distributed, fine-grained repair capability which will yield a significantly enhanced reliable performance over conventional approaches [8].

## 4 Conclusion

A self-repairing astrocyte-neuron network is proposed where a GABA interneuron is coupled with a tripartite synapse. This coupling facilitates a presynaptic

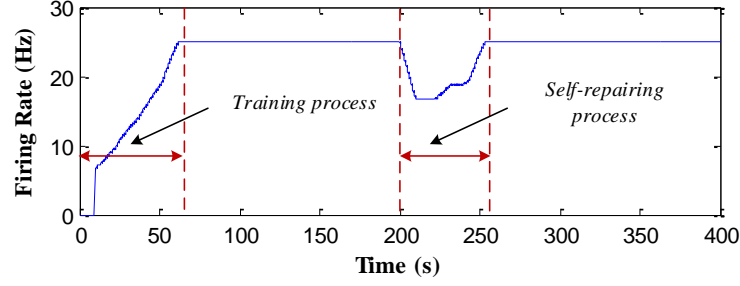


Fig. 6. Firing rate of N3 under the condition of partial faults.

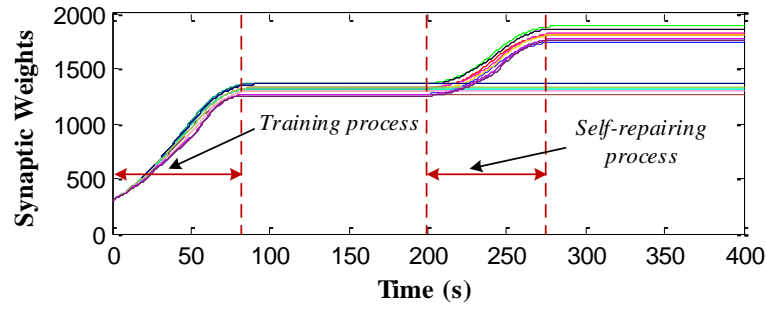


Fig. 7. Synaptic weights under the condition of partial faults.

frequency selectivity capability which can route input data, coded in spike trains, to different neuron within the S-ANN. Furthermore, the probability of release at tripartite synapses is modulated by both the pre and post synaptic frequency which provides a novel self-repairing learning rule which can learn new data patterns, assign them to neurons in the output layer and maintain this mapping in the presence of faulty connections between neurons. This self-repairing learning rule combines both the STDP and BCM rule and a plausible biophysical explanation for this was presented. Results presented demonstrate that when faults occur, the firing rate of post-synaptic neuron drops which re-opens the learning window and the S-ANN then re-trains to maintain the original input/output mapping. It was also shown that this mapping can be recovered for fault densities as high as 75% and future work will explore the biophysical under-pinning for this self-repairing capability and developed S-ANNs that can be applied to real world fault-tolerant application domains, e.g. robotics, automotive or aerospace.

**Acknowledgments.** This work is part of the EPSRC funded SPANNER project (EP/N007141X/1) (EP/N007050/1).



## References

1. Hu, J., Tang, H., Tan, K.C.: A hierarchical organized memory model using spiking neurons. In: International Joint Conference on Neural Networks. pp. 1–6 (2013)
2. McCarroll, N., Belatreche, A., Harkin, J., Li, Y.: Bio-inspired hybrid framework for multi-view face detection. In: International Conference on Neural Information Processing (ICONIP). pp. 232–239 (2015)
3. Liu, J., Harkin, J., McElholm, M., McDaid, L., Jimenez-Fernandez, A., Linares-Barranco, A.: Case study: Bio-inspired self-adaptive strategy for spike-based PID controller. In: IEEE International Symposium on Circuits and Systems (ISCAS). pp. 2700–2703 (2015)
4. Service, R.F.: The brain chip. *Science* 345(6197), 614–616 (2014)
5. Furber, S.B.: Brain-inspired computing. *IET Computers & Digital Techniques* pp. 1–7 (2015)
6. Stevens, B.: Neuron-astrocyte signaling in the development and plasticity of neural circuits. *Neurosignals* 16(4), 278–288 (2008)
7. Wade, J., McDaid, L., Harkin, J., Crunelli, V., Kelso, S.: Self-repair in a bidirectionally coupled astrocyte-neuron (AN) system based on retrograde signaling. *Frontiers in Computational Neuroscience* 6(76), 1–12 (2012)
8. Liu, J., Harkin, J., Maguire, L.P., McDaid, L.J., Wade, J.J.: SPANNER: A self-repairing spiking neural network hardware architecture. *IEEE Transactions on Neural Networks and Learning Systems* pp. 1–14 (2017)
9. Johnson, A.P., Halliday, D.M., Millard, A.G., Tyrrell, A.M., Timmis, J., Liu, J., Harkin, J., McDaid, L., Karim, S.: An FPGA-based hardware-efficient fault-tolerant astrocyte-neuron network. In: IEEE Symposium Series on Computational Intelligence. pp. 1–8 (2016)
10. Perea, G., Gómez, R., Mederos, S., Covelo, A., Ballesteros, J.J., Schlosser, L., Hernández-Vivanco, A., Martín-Fernández, M., Quintana, R., Rayan, A., Díez, A., Fuenzalida, M., Agarwal, A., Bergles, D.E., Bettler, B., Manahan-Vaughan, D., Martín, E.D., Kirchhoff, F., Araque, A.: Activity-dependent switch of GABAergic inhibition into glutamatergic excitation in astrocyte-neuron networks. *eLife* 5, 1–26 (2016)
11. Gerstner, W., Kistler, W.M.: Spiking neuron models: Single neurons, populations, plasticity. Cambridge University Press (2002)
12. Abbott, L.F., Nelson, S.B.: Synaptic plasticity: taming the beast. *Nature Neuroscience* 3, 1178–1183 (2000)
13. Song, S., Miller, K.D., Abbott, L.F.: Competitive Hebbian learning through spike-timing-dependent synaptic plasticity. *Nature Neuroscience* 3, 919–926 (2000)
14. Bienenstock, E.L., Cooper, L.N., Munro, P.W.: Theory for the development of neuron selectivity: Orientation specificity and binocular interaction in visual cortex. *The Journal of Neuroscience* 2(1), 32–48 (1982)
15. Bear, M.F., Cooper, L.N., Ebner, F.F.: A physiological basis for a theory of synapse modification. *Science* 237(4810), 42–48 (1986)